

# Photon Detection With Cooled Avalanche Photodiodes: Theory and Preliminary Experimental Results

D. L. Robinson and D. A. Hays  
Communications Systems Research Section

*Avalanche photodiodes (APDs) can be operated in a "geiger-tube" mode so that they can respond to single electron events and thus be used as photon counting detectors. Operational characteristics and theory of APDs while used in this mode are analyzed and assessed. Preliminary experimental investigation of several commercially available APDs has commenced, and initial results for dark count statistics are presented.*

## I. Introduction

There are basically two facets to an optical communications system for deep space, namely transmission and reception. The transmitter consists of a laser beam transmitted through a telescope, expanding the beam diameter and reducing its divergence, while the receiver consists of a receiver telescope collecting the light and focusing it onto a detector. In order to maximize the efficiency of the overall system, one must optimize both the laser and the detector. This article deals with the latter.

There are basically two types of detection schemes, direct and heterodyne. The former, as the name implies, directly receives the transmitted optical signal. In contrast, heterodyne detection combines the received signal with a local oscillator field so that the signal may be detected even under high-background-noise conditions. Schematic representations of direct and heterodyne detection receivers are illustrated in Figure 1(a) and 1(b), respectively. In applications with little or no background noise, such as communications with spacecraft in outer planet missions, direct detection systems can outperform their heterodyne counterparts (Ref. 11). The detection scheme of the cooled APD described herein would

be used under such low background conditions for single photon direct detection.

At planetary distances, the transmitted power is highly attenuated mainly due to beam divergence. Optimization of the system under such conditions necessitates the detection of light pulses containing only a few photons. In order to achieve this high degree of receiver sensitivity, we need to use photodetectors with internal gain that is sufficiently large to overcome the thermal noise of the receiver amplifier so that single photon counting is possible. In addition, the photodetector should have a very low intrinsic dark current level. Currently, photomultiplier tubes (PMT) are the only detectors capable of detecting such minimal energy levels. Internal gains in excess of  $10^6$  are readily available with PMTs. With a modest amount of cooling (to approximately 230 K [ $-40^\circ\text{C}$ ]) the dark current levels can be sufficiently reduced to less than 100 photoelectrons/sec. There are, however, two main drawbacks to PMTs. The first is their low quantum efficiency. The best PMTs available have only 20% quantum efficiency at  $\lambda = 0.8 \mu\text{m}$  (i.e., at that wavelength, only one photoelectron is produced on the average for each 5 photons impinging on the PMT faceplate). Secondly, since PMTs are packaged in

glass vacuum tubes and operated at higher voltages (in the kilovolt region), they are less attractive for applications requiring high reliability (i.e., space based optical communications) than solid-state photodetectors.

There is, however, a solid-state photodetector alternative to the PMT which has recently gained some attention. This solid-state alternative is the avalanche photodiode (APD) used in a geiger counter mode. Since the APD is a semiconductor device, it is potentially more reliable than a PMT. Furthermore, APDs have quantum efficiencies greater than 80% in the visible and near-infrared regions of the electromagnetic spectrum. In their common mode of operation they are biased below their avalanche breakdown voltage. However, the gain that they can thus provide (approximately 100) is not sufficient for single photon counting. Biasing the APDs at voltages beyond the avalanche breakdown where higher gains are obtainable is not possible at room temperature because of their relatively large values of dark current and excess noise (Refs. 10, 12). However, by cooling the APD to temperatures where the dark current becomes negligible it can be operated in a geiger counter mode. When the APD is used in this mode, it is biased above the avalanche breakdown, and a sustained avalanche is produced from almost every electron-hole pair generated. The effective internal gain of this process is very high ( $10^7$  to  $10^8$ ), making single photon counting possible. This, together with the high quantum efficiency, may make cooled APDs an attractive alternative to PMTs in most applications requiring detection of low-level optical signals. There are some problems associated with APDs operating in this mode, however, and overcoming these problems is a prerequisite towards fully realizing their advantages.

Even though there has been some investigation by several groups into some of the problems encountered when the APD is used in this mode of operation (Refs. 1-8), specific characteristics unique to the application of deep space optical communication need yet to be assessed and analyzed. Some of these characteristics will be addressed in the following text.

The following section discusses the theory and operational characteristics of the APD while operated in this geiger mode. Then, in Section III the experimental set-up along with results for several commercial APDs will be discussed. Finally, Section IV summarizes and concludes the article.

## II. Theory and Operational Characteristics

When an avalanche photodiode (APD) is cooled to reduce the number of thermally generated carriers, it can be biased

beyond its avalanche breakdown voltage (but below its dielectric [zener] breakdown voltage) for an extended period of time. Under such conditions, the APD will perform in a geiger mode as a single photon detector. While in this mode, an electron-hole pair (either photo or thermally generated) has a high probability of initiating a breakdown. When a breakdown occurs, the voltage across the diode drops to the avalanche breakdown voltage,  $V_B$ . This voltage drop is translated into an output pulse which is large enough for detection without any further amplification. In order to clear carriers from the high field region of the diode and quench this sustained avalanche, the bias voltage across the diode must be reduced below  $V_B$ . The diode can be subsequently rebiased above  $V_B$ , thereby permitting a new carrier to initiate another avalanche. The varying bias conditions (i.e., the drop in the bias voltage below the breakdown voltage during the avalanche and subsequent re-bias above the breakdown voltage) can be implemented by either a passive or an active quenching circuit. The passive quenching circuit is simply a resistor ( $\approx 100\text{ K}\Omega$ ) in series with the diode as shown in Fig. 2. The active quenching circuit (Ref. 7) is more complicated and involves various feedback loops as schematically shown in Fig. 3. Figure 4 illustrates the actual current-voltage curve of a cooled APD utilizing (a) a passive quenching circuit, and (b) an active quenching circuit (Ref. 7).

Specifically, referring to Figs. 4(a) and 4(b), we shall review various states of the APD while passively and actively quenched. During passive quenching, (Fig. 4[a]) the APD is reverse biased beyond the breakdown and waiting for a carrier to initiate an avalanche (1). Once a single carrier has initiated an avalanche, current flows in the APD (2). This avalanche current discharges the intrinsic capacitance of the APD resulting in a voltage drop (3) across the diode creating a detectable pulse that needs no amplification. The avalanche is then quenched (4) and recharged (1) through the load resistor above the breakdown voltage. As with the passive quenching, the active quenching (Fig. 4[b]) is biased beyond the breakdown voltage (1) waiting for a single carrier to initiate an avalanche. Once a single carrier initiates a breakdown (2) the circuit forces a fast transition by shifting the load line below the breakdown voltage (3). The circuit then forces a fast transition of recovery by shifting the load line above the breakdown voltage.

The main drawback of the passive quenching is its relatively long recovery time. Subsequent pulses may be detected during this recovery time. However, due to the transient conditions, detection efficiency is reduced, resulting in lower detection probability. Furthermore, the avalanche gain is lower since the bias is not fully reset, resulting in a lower pulse amplitude. This phenomenon was observed experimentally and will be described in the next section. By using the active

quenching circuit, this phenomenon can virtually be eliminated.

The sustained avalanche initiation probability is defined as the probability that a carrier initiates a current pulse that is limited only by the external circuit and not by the internal gain of the APD (which tends to be extremely large in this mode of operation). This APD avalanche initiation probability has been analyzed by McIntyre (Ref. 8) and Oldham, et al. (Ref. 3), above the breakdown voltage and shall be discussed next.

For an electron (hole) generated at position  $x$  within the active region of an APD, the probability,  $P_e(x)$  ( $P_h(x)$ ), that an avalanche will be initiated can be calculated from the following formulas (Ref. 8):

$$-\log [1 - P_h(0)] = \frac{k}{1-k} \log [P_h(0)f(w) + 1 - P_h(0)] \quad (1)$$

$$1 - P_h(0) = [1 - P_e(w)]^k \quad (2)$$

where the boundaries of the avalanche region are  $x = 0$  and  $x = w$ , as illustrated in Fig. 5. The ionization coefficient ratio has been defined as  $k = \alpha_h/\alpha_e$  where  $\alpha_h(x)$  and  $\alpha_e(x)$  are the hole and electron ionization rates respectively. The parameter  $f(w)$  is defined as follows:

$$f(w) = \exp [(1-k)\delta]$$

$$\delta = \int_0^w \alpha_e(x) dx$$

$P_h(0)$  and  $P_e(w)$  are plotted in Fig. 6 for various values of  $k$  (Ref. 8). The ideal operational conditions of the APD require high probability of detection while minimizing the over bias. (Minimal over bias is preferred to minimize dark counts.) By inspection of Fig. 6, these conditions are optimized for values of  $k$  close to unity. It is to be noted that higher asymmetric values of  $k$  are preferred for the APD when operating in its normal mode (Ref. 10). Since commercially available APDs are not optimized for the requirements of the APD while operating in the cooled geiger mode, we can expect to achieve better performance with the APDs that have been optimized for cooled detection.

The main problem, however, with the APD used in this geiger mode is the occurrence of false avalanches. When an avalanche is initiated, it is possible for some of the avalanching charge carriers to be trapped. This may be caused by defects or impurities in the crystal lattice. At a later time after the bias is reset, these trapped carriers may be released causing

a secondary or false avalanche. These secondary avalanche processes may occur from several nanoseconds after the initial pulse to as long as minutes after the initial pulse (Ref. 6). The uncertainty of the time of these false events complicates the detection probability statistics. A theoretical model for the count statistics of a cooled APD has been created (Ref. 9). This model considers the APD output as a Poisson distributed primary avalanche process, plus a conditionally Poisson distributed process due to trapped-carrier induced secondary events. This model is the theoretical basis against which the experimental measurements will be compared.

### III. Experimental Verification

#### A. Experimental Set-up

The experimental set-up is depicted in Fig. 7. The APD is cooled with a Joule Thompson Micro Miniature Refrigerator (MMR) System I. The cooler consists of an evacuated chamber with a cold finger on which the diode is mounted. Optical access to the diode is provided by a glass port. Neutral density filters can be used to control the amount of light impinging on the APD. A beam splitter diverts part of the beam to a PMT to calibrate incident detected photon intensities. An HP 5370A counter and HP 85 desktop computer are utilized for data acquisition and analysis. A storage oscilloscope (Tektronix 7834) is utilized to view individual waveforms and time intervals between successive pulses. The entire optical portion of the experiment is enclosed in a light-tight, dark enclosure.

#### B. Experimental Preliminary Results and Discussions

Experimental results in this report include only dark count measurements with the passive quenching circuit. The second phase of our experiment will analyze signal detection with the passive quenching circuit. Finally, the active quenching circuit will be incorporated into the experimental set-up.

Dark count noise characteristics of Si APDs have been evaluated from three manufacturers (Mitsubishi Model #PD1002, NEC Model #NDL1202, and RCA Model #C30817). Initial measurements were made without incident light in order to characterize the dark counts and gain some insight into some of the possible physical processes occurring in the device.

First, the dark count characteristic of each of the diodes as a function of temperature was characterized in order to determine the optimum operating temperature range. All experimental testing reported in the literature (Refs. 1-7) has been performed on cooled Si APDs at 77 K only. In our experimental apparatus, the temperature of the refrigerator is controllable from approximately 79 K to 390 K. The dark count

frequency was measured over 60-sec time intervals and at various temperatures from 79 K to room temperature. Results are graphed in Figs. 8(a) and 8(b) for the diodes tested. As the temperature was increased, the reverse breakdown voltage also increased as expected (Ref. 10) (see Figs. 8[a] and 8[b]).

Aside from the increased breakdown voltage at higher temperatures, the number of counts at a given voltage increment above breakdown remains fairly constant from 79 K to 180 K for the diodes tested. Stated differently, the performance of the diode does not degrade significantly over this temperature range. Since multistage, thermoelectric coolers operated in evacuated environments are capable of operation down to approximately 140 K, they could be useful in cooling the APDs in space applications. At temperatures greater than 180 K, the number of dark counts generated greatly increased making the APD unusable as an efficient communications detector in this mode of operation.

Next, we characterized dark counts of each diode as a function of reverse bias voltage (above the breakdown voltage of the cooled APD). The goal was to determine the relative performance of the APDs from different manufacturers. We saw in the previous section that as the reverse bias is increased, the probability of breakdown is increased, resulting in higher dark counts. However, since the amplitude of the output pulse from the cooled APD is also a function of this reverse bias, there are some definite trade-offs between the output signal amplitude and increased dark current due to higher bias levels when the APD is used to detect actual signal. Of the two APDs tested, Mitsubishi Model No. PD1002 had the best performance with the least number of counts for the greatest range of voltage above breakdown.

During the recovery time of the circuit after an avalanche has occurred, subsequent avalanches are still possible but with reduced probability since the bias is not fully recharged. Figure 9 illustrates this phenomenon of secondary avalanches prior to full recovery of the reverse bias voltage. At point "A" of Fig. 9, the APD is biased  $\sim 0.5$  volts above breakdown. Then, at point "B," a carrier initiates an avalanche causing a voltage drop to point "C." For approximately 400  $\mu$ s after this voltage drop, avalanches continue to occur prior to full recovery of the circuit at point "D." Upon full recovery, another carrier initiates an avalanche at point "E" resulting in a sub-

stantial voltage drop. This time, however, the circuit fully recharges after the initial breakdown at point "E." As the circuit is recharged to its full value the probability of breakdown increases accordingly.

Finally, the statistics of the interarrival times between pulses were examined to gain some insight into the noise mechanism statistics and to try to determine if trapping or secondary pulses are a significant component of the noise. The time interval between the pulses was measured with the HP 5320 counter. Measurements were taken at various thresholds and reverse bias voltages. Histograms of the time interval data for the two diodes tested are graphed in Figs. 10(a) and 10(b).

The Chi-square goodness of fit test was used to determine whether the observed dark counts were Poisson distributed (i.e., exponential pulse interarrival times). In spite of the various parameters that we tried to fit the experimental data to, the results indicate that unlike the PMT (Ref. 13), and unlike the results reported on cooled APDs elsewhere (Ref. 6), the dark counts in this case do not seem to be Poisson distributed. The data from the two diodes seemed to have too many short interarrival counts and too long a tail of the distribution curve to be Poisson. This may be due to the secondary emission "detrapping" effects of the APD or may be a result of the long recovery time from the passive quenching circuit. The latter effect would be eliminated using the active quenching circuit. Both effects are currently under investigation.

## IV. Conclusion

Photon counting with cooled APDs operating in the geiger counter mode may be an attractive alternative to PMTs. An initial investigation of the theory and operational characteristics of the APDs used in this mode for single photon detection has been completed. Experimental investigation of several commercial APDs has commenced, and initial results for dark count statistics have been presented. Further investigations of "trapping" effects have yet to be performed to determine their impact on detection probabilities and hence the value of using the cooled APD as a detector for optical communications. The next phase of the experimental program will include a performance evaluation of the noise signal detection probability which will be compared to the theory presented herein.

## Acknowledgment

The authors wish to thank Joe Katz for many helpful discussions and for his critical review of this paper.

## References

1. Webb, P. O. and McIntyre, R. J., "Single Photon Detection with Avalanche Photodiodes," *Bull. Amer. Phys. Soc.*, Ser II, 15, p. 813 (1970).
2. Haecker, W., Groezinger, O., and Pilkun, M. H., "Infrared Photon Counting by Ge Avalanche Diodes," *Appl. Phys. Lett.* 19, pp. 113-115 (1971).
3. Oldham, W. G., Samuelson, R. R., and Antognetti, P., "Triggering Phenomena in Avalanche Diodes," *IEEE Trans. Electron Dev.* ED-19, pp. 1056-1060.
4. Ekstrom, P. A., "Triggered-Avalanche Detection of Optical Photons," *J. Appl. Phys.* 52, pp. 6974-6979 (1981).
5. Cova, S., Longoni, A., and Ripamonti, G., "Active-Quenching and Gating Circuits for Single-Photon Avalanche Diodes (SPADs)," *IEEE Trans. Nucl. Sci.*, NS-29, pp. 99-601 (1982).
6. Ingerson, T. E., Kearny, R. J., and Coutler, R. L., "Photon Counting with Photodiodes," *Appl. Opt.*, 22, pp. 2013-2018 (1983).
7. Cova, Sergio, et al., "A Semiconductor Detector for Measuring Ultraweak Fluorescence Decays with 70 ps FWHM Resolution," *IEEE Journal of Quantum Electronics*, QE-19, No. 4, April 1983.
8. McIntyre, Robert, "On the Avalanche Initiation Probability of Avalanche Diodes Above the Breakdown Voltage," *IEEE Transactions on Electron Devices*, ED-20, No. 7, July 1973.
9. Tan, H. H., "Avalanche Photodiode Statistics in Triggered-Avalanche Detection Mode," *TDA Progress Report 42-79*, Jet Propulsion Laboratory, Pasadena, CA, July-September 1984, pp. 69-80.
10. Sze, S. M., *Physics of Semiconductor Devices*, (John Wiley and Sons, Inc., New York, 1981), Chapter 13.
11. Lesh, J. R., "Optical Communications Research to Demonstrate 2.5 bits/detected photon," *IEEE Communications Magazine*, Nov. 1982, pp. 35-37.
12. Katz, J., "Detectors for Optical Communications: A Review," *TDA Progress Report 42-75*, Jet Propulsion Laboratory, Pasadena, CA, July-September 1983, pp. 21-38.
13. Lesh, J. R., et al., "2.5/Detected Photon Demonstration Program: Description, Analysis, and Phase I Results," *TDA Progress Report 42-66*, Jet Propulsion Laboratory, Pasadena, CA, September-October 1981, pp. 115-132.

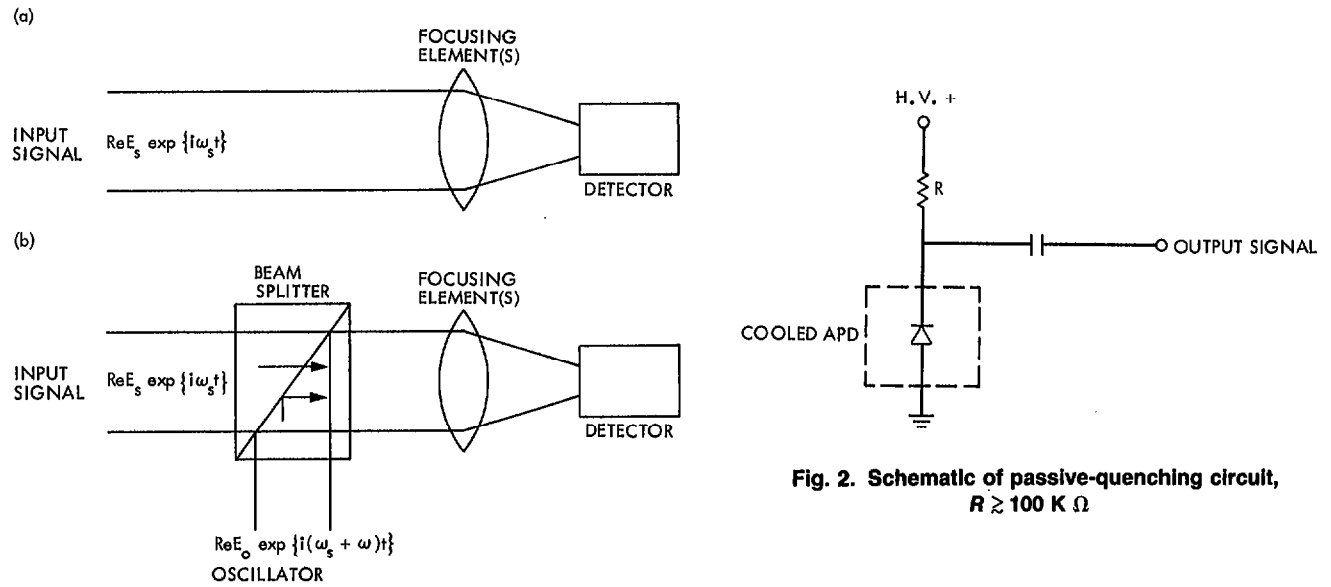


**Fig. 2. Schematic of passive-quenching circuit,**  
 $R \gtrsim 100 \text{ K } \Omega$

**Fig. 1. Schematic representation: (a) direct detection scheme used in optical communication under low background conditions; (b) heterodyne detection scheme used in optical communication under high background conditions**

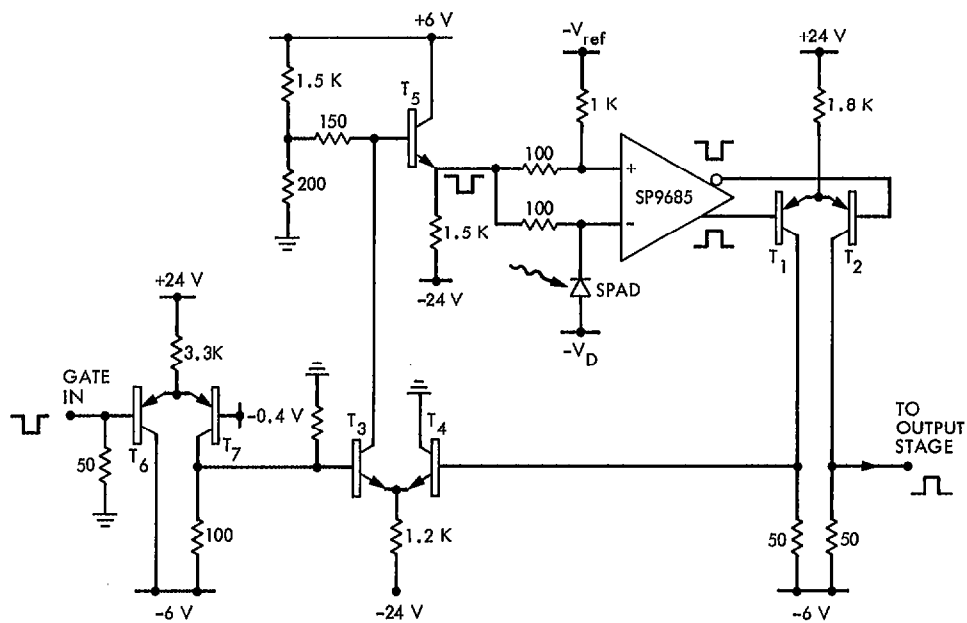


**Fig. 3. Diagram of active-quenching circuit (adapted from Ref. 7)**

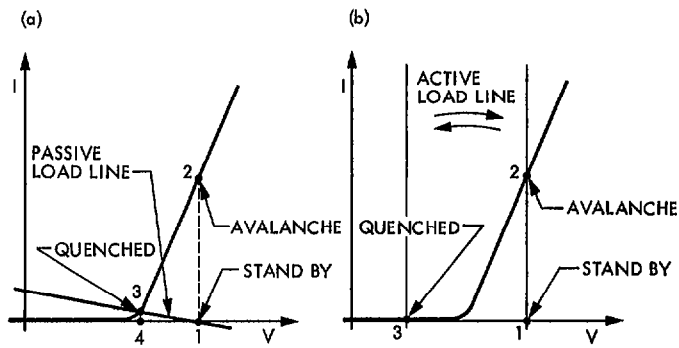


Fig. 4. Cooled APD current-voltage curve during (a) passive quenching and (b) active-quenching. See text for explanation of specific states (adapted from Ref. 4).

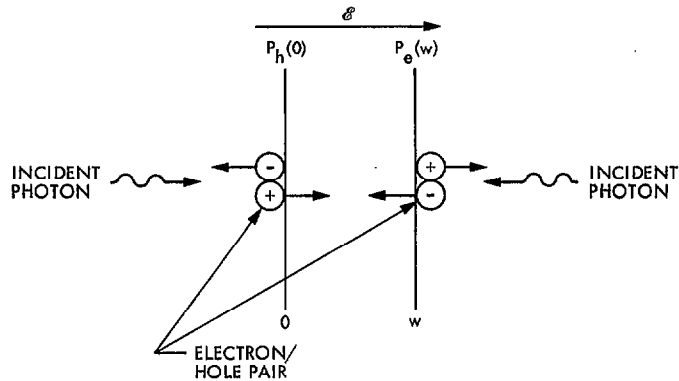


Fig. 5. Schematic representation of photon interaction with an electron/hole pair for an active region of length  $w$ . The quantity  $\xi$  is the applied electric field.

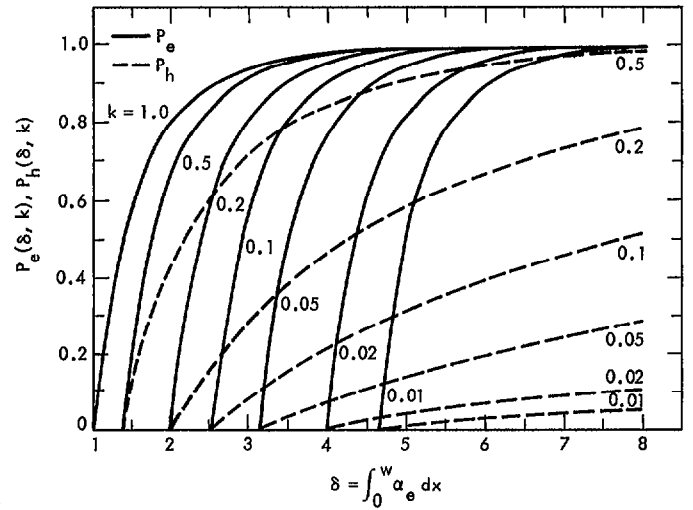


Fig. 6. Avalanche initiation probability by an injected electron ( $P_e$ ) or hole ( $P_h$ ) as a function of the electron ionization coefficient (adapted from Ref. 8)

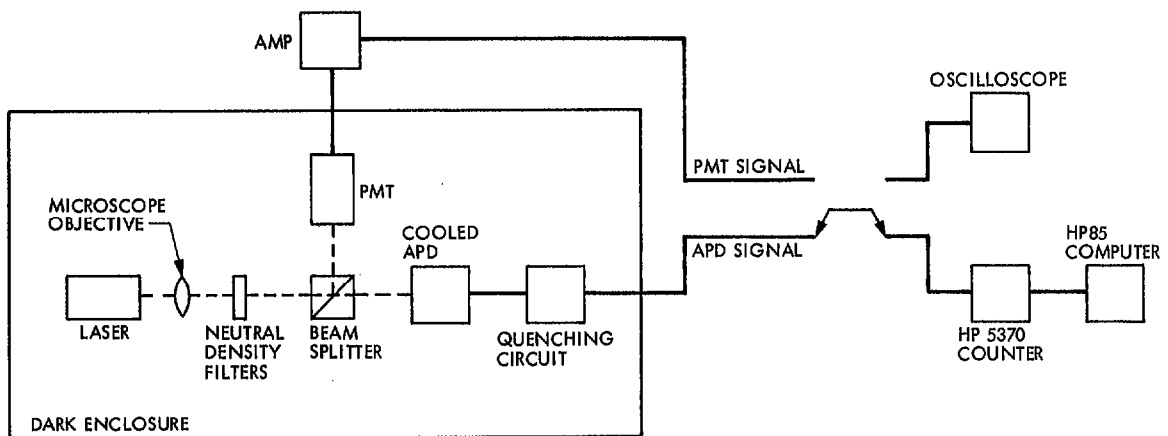
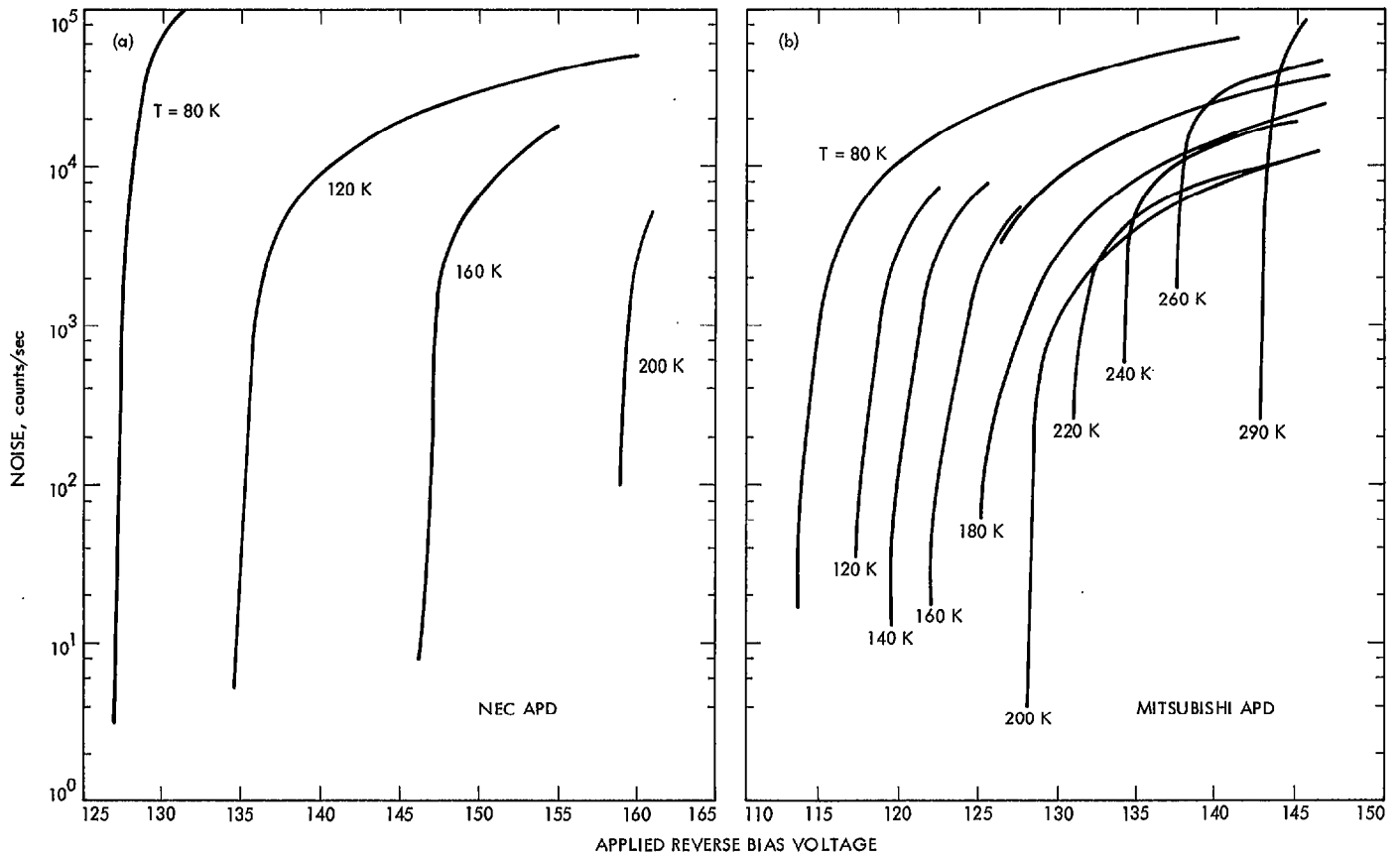
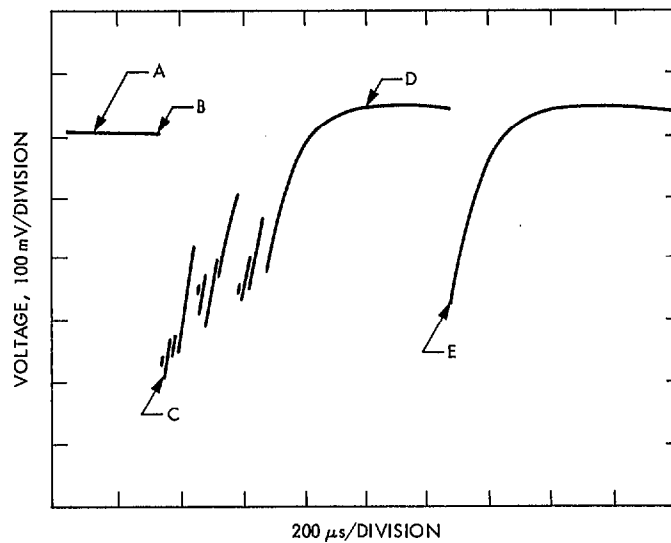


Fig. 7. The cooled APD experimental set-up. A PMT is used to calibrate light intensity from the GaAlAs laser.



**Fig. 8. Dark counts per second of the cooled (a) NEC (Model NDL 1202) APD and (b) Mitsubishi (Model No. PD1002) APD are graphed as a function of temperature and reverse bias voltage**



**Fig. 9. Oscilloscope trace of output pulses from cooled NEC Model No. NDL1202 APD with passive quenching circuit. APD has been bias  $\sim 0.5$  V above breakdown. Note secondary breakdown of diode before circuit has fully recharged. Temperature = 200 K, applied bias voltage = 160 V.**



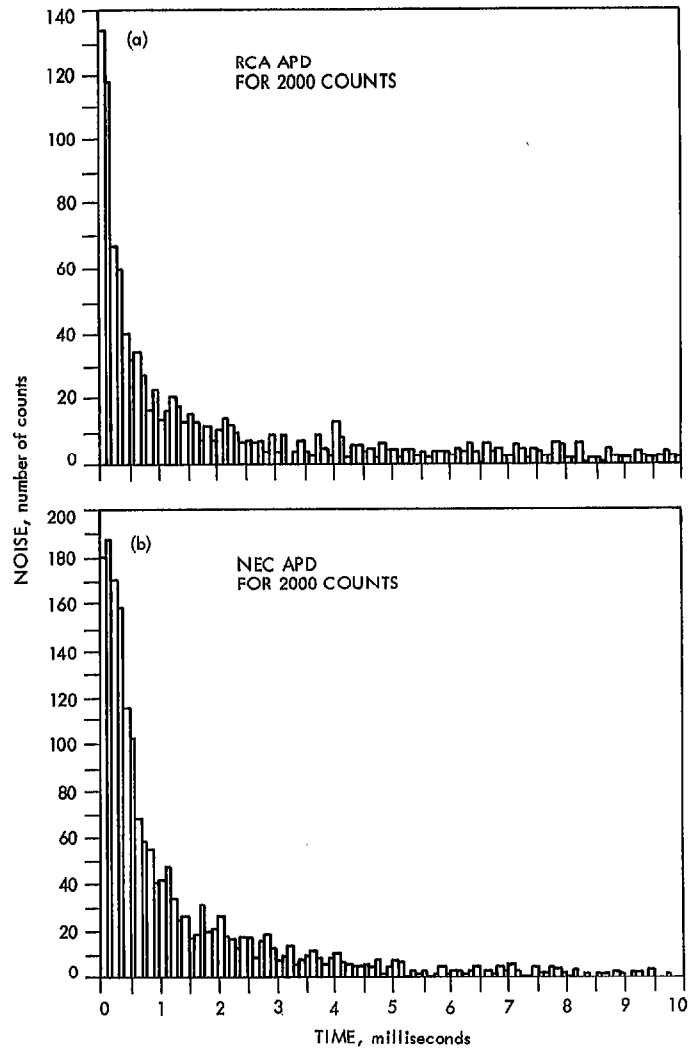


**Fig. 10. Histogram of time interval arrival times for: (a) RCA Model No. C30817. Temperature = 80.7 K, applied bias voltage = 117 V; (b) NEC Model No. NDL1202. Temperature = 88.6 K, applied bias voltage = 129.4 V.**